Sentinels4Carbon (Sense4Fire)

Sentinel-based fuel, fire and emissions products to constrain the changing role of vegetation fires in the global carbon cycle

ESA Contract Number: 4000134840/21/I-NB

Product Validation Report Version 3

(PVRv3)

3 May 2024, Version 3

Prepared by:

Matthias Forkel, Daniel Kinalczyk, Christine Wessollek, Christopher Marrs

Technische Universität Dresden, Faculty of Environmental Sciences, Dresden, Germany

Vincent Huijnen, Jos de Laat

Royal Netherlands Meteorological Institute (KNMI), De Bilt, The Netherlands

Niels Andela, Dave van Wees

BeZero Carbon Ltd., London, UK

Contents

Figures

Figure 1: Comparison of different fuel components for the Cerrado biome from three different satellite-based approaches. Please note that WDfuel in L22 includes woody biomass for trees with diameter at breast height > 10 cm while TUD.S4F treats shrubs as small trees. SUfuels in L22 includes all dead herbaceous and woody plant material at the

Tables

1 Introduction

This Product Validation Report version 3 (PVRv3) describes results of the validation and inter-comparison of products from the three approaches applied in Sense4Fire to estimate fire emissions, fuel loads and fuel consumptions.

The validation of data products is crucial for the evaluation of the complex production chain underlying the Sense4Fire project: That is, algorithms that combined data from either Sentinels into data products, algorithms that merge those data products into emissions, IFS-COMPO model simulations that use those emissions to simulate the spatio-temporal structure of the chemical composition of the atmosphere, and Sentinel-5p atmospheric composition data that is used to validate and re-calibrate those model simulation results. Differences between the IFS-COMPO model simulation and Sentinel-5p observations thus can be caused by one of the many processes in the Sense4Fire production chain. Hence the validation should not only focus on the comparison between model results and Sentinel-5p data, but also on the validation of individual data products further down the production chain. Understanding and quantifying errors and uncertainties is important to identify where and when the production chain can be improved. The validation may lead to immediate data product improvement, but equally to identification of data product limitations that cannot be immediately resolved and require additional action. The latter will find its way into a gap analysis that will be part of the PVR and final project report. The gap analysis can be used to initiate or support additional research and development activities beyond the Sense4Fire project end.

PVRv3 builds on the description of methods and algorithms from the Algorithm Theoretical Baseline Document version 2.1 (ATBDv2.1) (Forkel et al., 2023) and the updates described in ATBDv3 (Forkel et al., 2024).

2 Validation approach

Sense4Fire provides two bottom-up fire emission approaches (GFA-S4F and TUD-S4F) and a set of approaches (summarised as KNMI-S5p) to provide a top-down benchmark of the estimated fire emissions:

- The **GFA-S4F** approach is based on the Global Fire Atlas (GFA) algorithm (Andela et al., 2019, 2022) and uses observations of active fires from the VIIRS and Sentinel-3 SLSTR instruments with a new fire type map to estimate fire emissions.
- The **TUD-S4F** approach is a data-model fusion approach that combines several datasets from Sentinel-3 and other Earth observation products to estimate fuel loads, fuel moisture, fuel consumption, and fire emissions.
- The set of **KNMI-S5p** approaches as introduced in PVRv2.1 explored the use of Sentinel-5p TROPOMI data (NO_2, CO) to assess bottom up emission estimates. This includes one example of a post-hoc scaling approach for CO.

This PVR provides validation results for each study region separately, as the different study regions were processed independently from each other and differ in some cases with respect to the used input data (see ATBDv3). For each study region, we first provide validation results that are specific for the GFA-S4F and TUD-S4F approaches and then provide a comparison against the Sentinel-5p based benchmark (KNMI.S5p).

The methods and approaches for evaluation and validation using Sentinel-5p TROPOMI data have been explored and described in PVR2.1 and ATBDv2.1 as well as in de Laat et al. (2024). In summary, those methods and approaches have been assessed as appropriate and valuable for assessing and benchmarking bottom-up wildfire emission databases. In this PVR their use has been expanded to all regions originally defined within Sense4Fire while a new region has been added (Europe) and the time period for which results are analysed has been expanded (entire year 2020).

In brief, in the KNMI.S5p benchmarking activities, bottom-up emissions are used as input for atmospheric chemistry model simulations using the IFS-COMPO model. The model output is collocated with cloud free TROPOMI observations including application of observation operators like the averaging kernel. The comparison dataset is then further analyzed and (dis)agreement between TROPOMI data and model results provide less or more confidence in the realism of the bottom-up emissions.

In addition, the previous PVRv2.1 also introduced an innovative approach using model results for a post-hoc adjustment of the bottom-up NO_x emissions, the so-called β-approach (see also the ATBDv2.1). Differences in tropospheric NO_2 columns between two model simulations – one with the bottom-up emission of choice and one with modified bottom-up emissions, in our case a 20% NO_x emission decrease – provide the local sensitivity of the bottom-up emissions to differences in tropospheric NO_2 columns. This relationship is then used to translate differences in TROPOMI observed and IFS-COMPO tropospheric NO_2 columns to differences in the bottom-up emissions.

Although there are some caveats and limitations to this method, it does provide at minimum a sanity check on the bottom-up emissions: small differences in emissions before and after β-correction provide confidence in the bottom-up emissions that were used. Large differences indicate less reliable emissions. Furthermore, multiple bottom-up emission database may differ significantly in their prior emission estimates. If after β-correction emissions are closer together then this is a good indicator that there are sufficient TROPOMI observations to constrain the bottom-up emissions. Likewise, continued large differences in emissions after β-correction indicate that there are insufficient TROPOMI observations to constrain emissions.

3 Amazon and Cerrado

3.1 Validation of GFA-S4F

We have not revised our approach or validation for the Amazon and Cerrado regions since the PVR2.1.

3.2 Validation of TUD-S4F

Several validation exercises were performed for the South America study region. We compared estimated fuel loads with two other datasets, estimated emission factors were compared with the compilation of emission factors by Andreae et al. (2019) and finally estimated emissions were compared with KNMI-S5p, GFA-S4F and GFAS (Kaiser et al., 2012).

3.2.1 Comparison of fuel loads

Estimated fuel loads were compared with two other satellite based estimates, namely from the GFED500m model (van Wees et al., 2022) and with the estimates by Leite et al. (2022). GFED500m uses a simplified version of the CASA biogeochemical model to estimate net primary production, carbon turnover and then the accumulation and decay of surface fuels. Leite et al. (2022) (L22) performed field measurements of fuels in the Cerrado and applied machine learning models to estimate fuel loads over larger areas by taking information from the GEDI space-borne Lidar as predictors.

Spatial patterns and absolute values of estimated surface fuel loads are different between the three approaches (Figure 1). TUD-S4F shows similar spatial patterns and absolute values of leaf and woody biomass with GFED500m but differs in comparison with L22. In L22, woody biomass is generally lower. The magnitude of woody debris in TUD-S4F is similar to GFED500m and L22 but spatial gradients are especially different with L22. The larger difference of TUD-S4F and GFED500m with L22 is likely caused by the used field data in L22 which was mainly taken in the eastern Cerrado which is dominated by herbaceous fuels. *In situ* measurements from the Amazon show a range of CWD from 2.2 to 9.3 kg/m² (Scaranello et al., 2019), which corresponds to the range in the TUD.S4F approach. Those comparisons of surface fuels indicate that TUD-S4F produces estimates within plausible ranges, however, a proper validation of surface fuel loads requires more field observations.

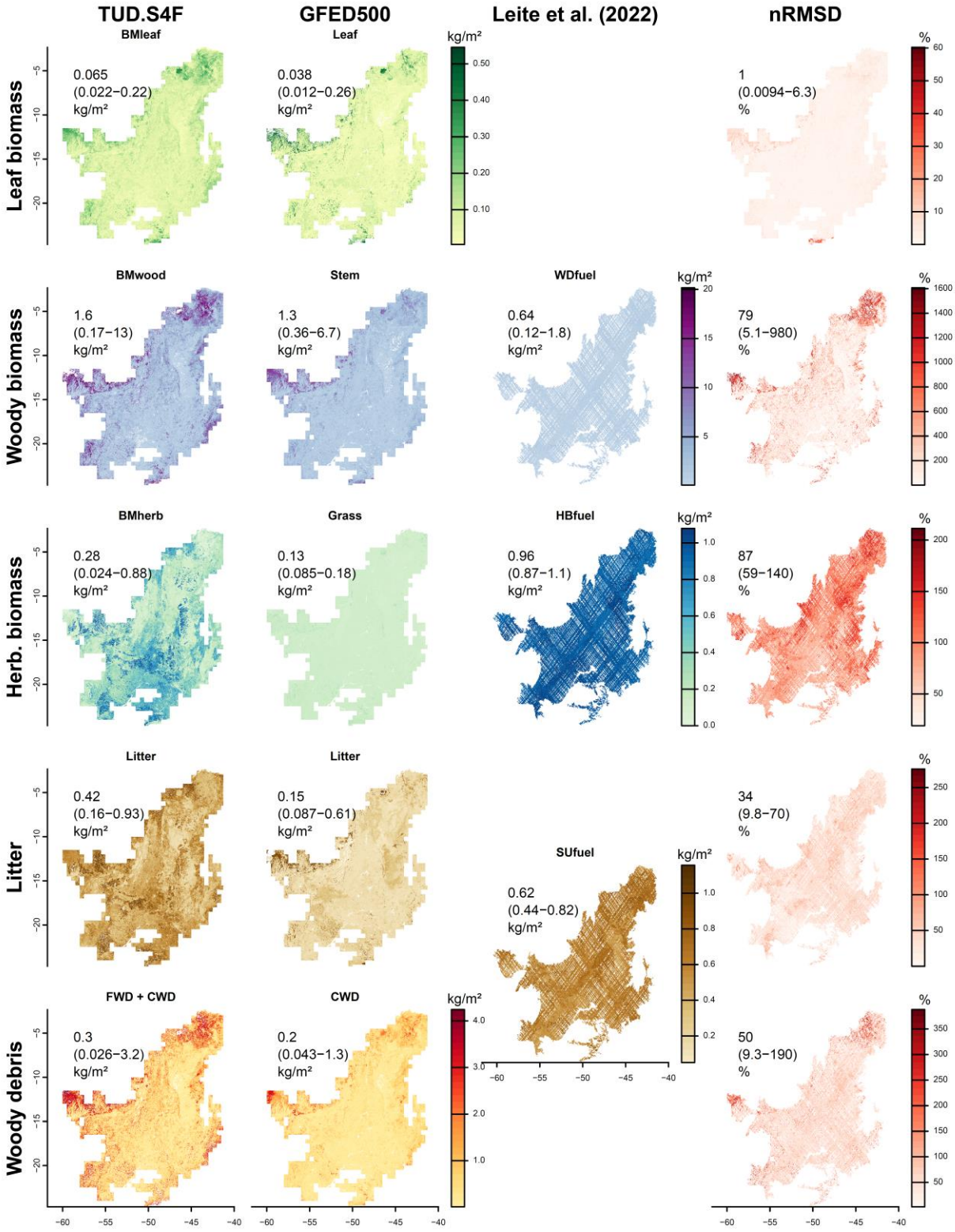

Figure 1: Comparison of different fuel components for the Cerrado biome from three different satellite-based approaches. Please note that WDfuel in L22 includes woody biomass for trees with diameter at breast height > 10 cm while TUD.S4F treats shrubs as small trees. SUfuels in L22 includes all dead herbaceous and woody plant material at the surface and hence a direct assignment of SUfuel to the litter or woody debris classes in TUD.S4F and GFED500m is not possible. nRMSD is the normalized root mean squared difference relative to the mean value of the three approaches. The numbers in each map represent the median value and percentiles 5% and 95% of the values in each map.

3.2.2 Comparison of emission factors

The dynamically estimated modified combustion efficiency (MCE) and emission factors (EF) in TUD-S4F were calibrated against the data for tropical forests and savannas by Andreae et al. (2019) (A19). Figure 2 shows the distribution of MCE and EFs from A19 and from TUD-S4F prior to the calibration (S4F-pri) and after calibration (S4F-opt).

Consistent with A19, TUD.S4F also yields higher modified combustion efficiency (MCE) and hence more flaming combustion in savanna fires than in deforestation and forest fires and hence reproduces the statistical distribution by A19.

We estimate a variability of the emission factor for CO (EF_{CO}) from savannas (minimum 40 g/kg) to forests (maximum 120 g/kg), which aligns well with the mean and variability of EF_{CO} reported by A19 (Figure 4b). TUD-S4F agrees with A19 in the median emission factor for CO_2 but shows a slightly larger variability. TUD-S4F seems to underestimate the emission factor for PM2.5.

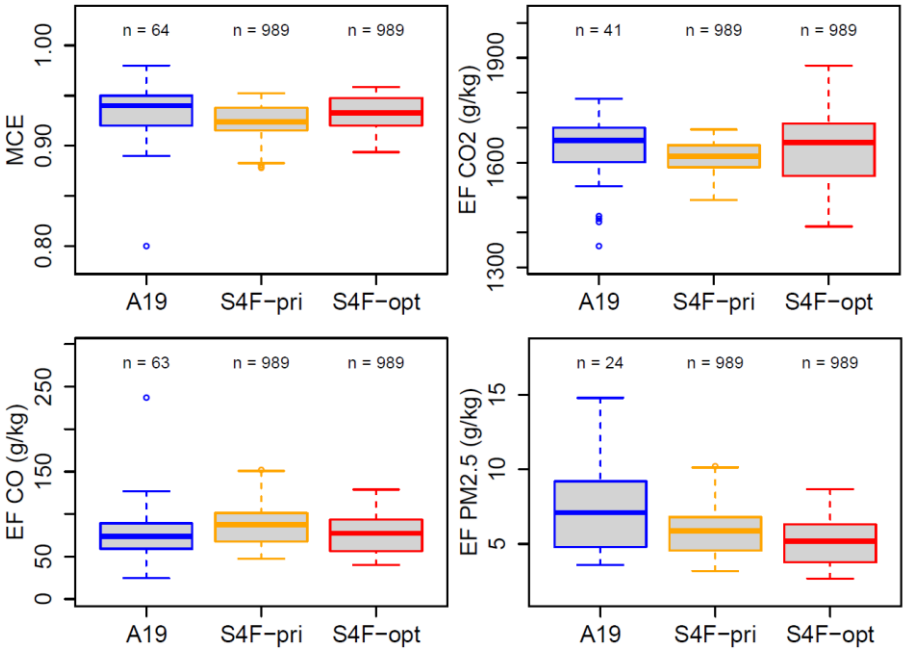

Figure 2: Comparison of modified combustion efficiency and emission factors from Andrea (2019) (for tropical forests and savannas) with results from TUD-S4F prior and after optimization for the Amazon and Cerrado.

3.2.3 Comparison of estimated emissions

Emissions from TUD-S4F have been compared against the top-down benchmark estimates from Sentinel-5p (Figure 3) and with the estimates from GFA-S4F. We found that regional total CO and NOx emissions agree well with KNMI-S5p if TUD-S4F is applied with dynamic emission factors and the GFA-S4F burned area estimates. When run with medium resolution burned from Fire CCI or with fixed emission factors, emissions are underestimated (Table 1). For individual fire types, TUD-S4F shows higher emissions for savannah fires but lower emissions for deforestation fires than KNMI-S5p. However, those

results should be taken with caution as KNMI-S5p cannot well resolve sub-regional and local features of fire emissions (especially for CO).

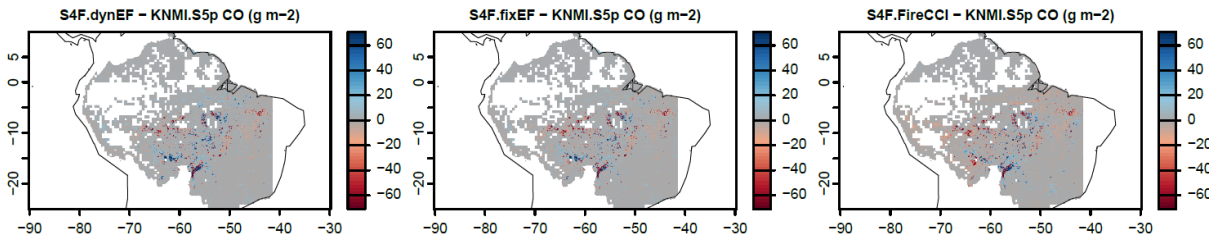

Figure 3: Difference in total CO emissions for the period 1st August - 31st October 2020 between the three estimates with TUD-S4F and the estimates derived from Sentinel-5p.

Table 1: Fire emissions of CO (Tg CO) and NO_x (Tg NO) for each approach aggregated for different fire types over the Amazon and Cerrado for the period 1st August – 31st October 2020.

Species	Approach	Savanna	Clearing	Forest	Deforest.	Total
CO	TUD.S4F	13.85	5.04	15.62	9.20	43.73
CO	TUD.S4F.fixEF	12.51	4.08	12.66	7.38	36.64
CO	TUD.S4F.FireCCI51	12.35	1.20	9.57	6.62	29.75
CO	GFA.S4F	9.81	3.06	15.7	13.06	41.64
CO	KNMI.S5p	10.21	2.97	15.13	15.24	43.56
NO	TUD.S4F	0.34	0.11	0.33	0.19	0.97
NO	TUD.S4F.FireCC51	0.32	0.03	0.20	0.14	0.69
NO	GFA.S4F	0.30	0.07	0.3	0.24	0.91
NO	KNMI.S5p	0.30	0.07	0.23	0.27	0.87

3.3 Validation against Sentinel-5p

The main focus of the previous PVRv2.1 has been on the Amazon/Cerrado region and used the GFAS emissions as prior for a relatively short period of time (August-September 2020). The main findings for that region, relevant to this work, were (1) the presence of a so-called "large fire NO_x bias" in the bottom-up emissions, and (2) a general underestimation of fire CO emissions in GFAS (de Laat et al., 2024).

Although the differences for the large fires were found very significant, for the total budget of fire NOx emissions in the region they turned out be of less importance, *i.e.* the

total NOx budget is dominated by the many small(er) fires. In contrast, the fire CO emissions in GFAS were underestimated, which was shown to be a consistent feature not only in the Amazon/Cerrado region but also in south-equatorial Africa, Siberia as well as western USA.

For the Amazon/Cerrado region, the post-hoc β-method also resulted in significant changes in fire NO_x emissions and subsequently a better agreement between IFS-COMPO simulations using the post-hoc emissions and TROPOMI observations of tropospheric NO_2 over the fire region.

This update/extension of the PVR builds on those results by extending the analysis to all selected regions as well as a new region (Europe/Mediterranean) and by extending the simulations to an entire year (2020). The main bottom-up emission databases used are GFAS and GFA-S4F, but some results from the β-optimization and using emissions from the TUD-S4F will also be presented and discussed. Note that the GFAS emission used here are from a preliminary re-processed GFAS version (GFAS experiment ID "i1j7") that may contain small differences in the GFAS emissions as used for the PVRv2.1 and also in de Laat (2024).

The time series of daily emissions (Figure 2.3.1) shows consistent variations for both GFAS and GFA-S4F with a strong peak in September 2020 (day of year 250-270). The total NOx emission estimates for 2020 are quite comparable, although somewhat lower for GFAS (77 Gg) than GFA-S4F (109 Gg).

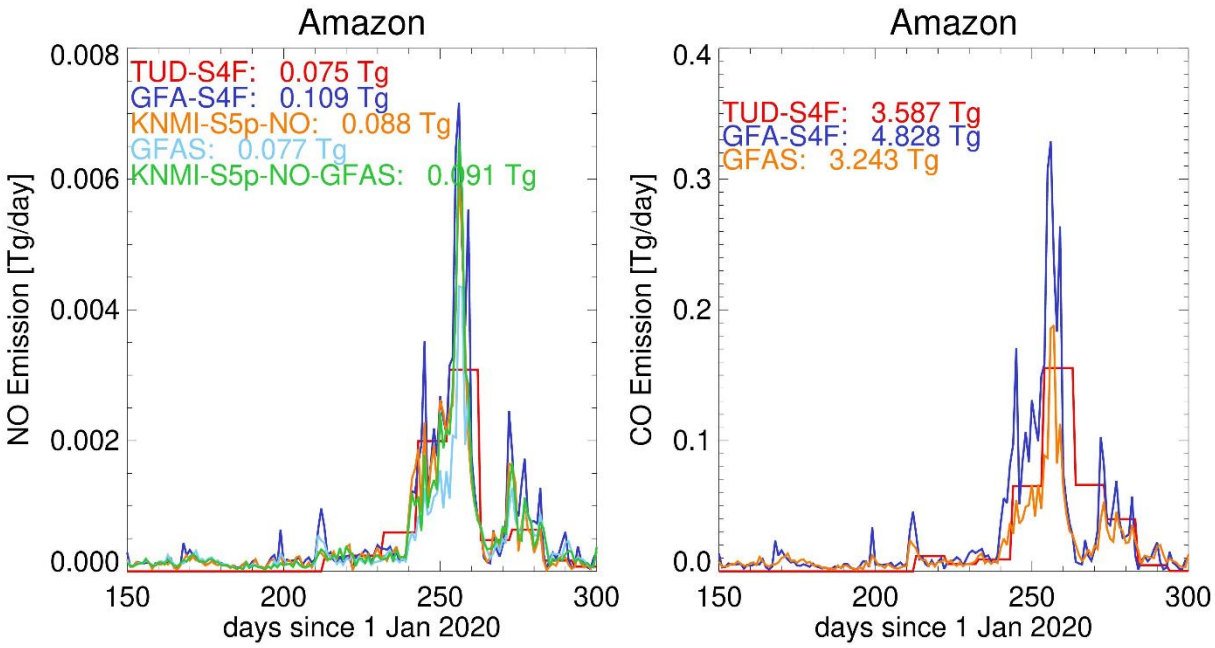

Figure 4: Time series of June-October 2020 daily NOx emissions (left panel) and daily CO emissions (right panel) for the Amazon/Cerrado region. The emissions are displayed for both the GFAS and GFA-S4F emissions as well as for NOx the associated β-optimized emissions.

Results using the GFAS emissions (Figure 4, left panel) show in general a fair agreement between observed and modeled tropospheric NO_2 columns although the regression indicates an underestimation which is dominated by the distribution and dominance of smaller tropospheric NO_2 columns ($5 < 10^{15}$ molecules cm^{-2}). There is less evidence of a large-fire NO_x bias in these GFAS emissions, unlike previously reported results (PVR v2 and (de Laat et al., 2024)). However, there is a large spread in the distribution around the 1:1 line.

The distribution for the GFA-S4F simulations (Figure 4, right panel) are quite similar to those of GFAS but with a clearer large-fire NO_2 bias (there are data points outside the y-axis range, not shown here). The regression results are closer to the 1:1 line (regression coefficient 1.19) but the binning-regression indicates that the regression results are rather sensitive to the choice of regression (regression coefficient 1.95) which is related the non-gaussian distribution of data points.

Results for individual months – not shown – are rather similar for both IFS-COMPO simulations. They also indicate that the differences in regression are purely the result of differences in fire emissions (July-October) as for the non-fire months regression values between both are very similar.

When optimizing the NO_x emissions with respect to TROPOMI NO_2 observations using the β-method we reach nearly identical values independent of the a-priori emissions (91 Gg $yr^{-1}$and 88 Gg yr^{-1}, see Figure 4). These results reveal a rather consistent picture for the Amazon/Cerrado region for all available databases and approaches and provide confidences in the NO_x emission estimates.

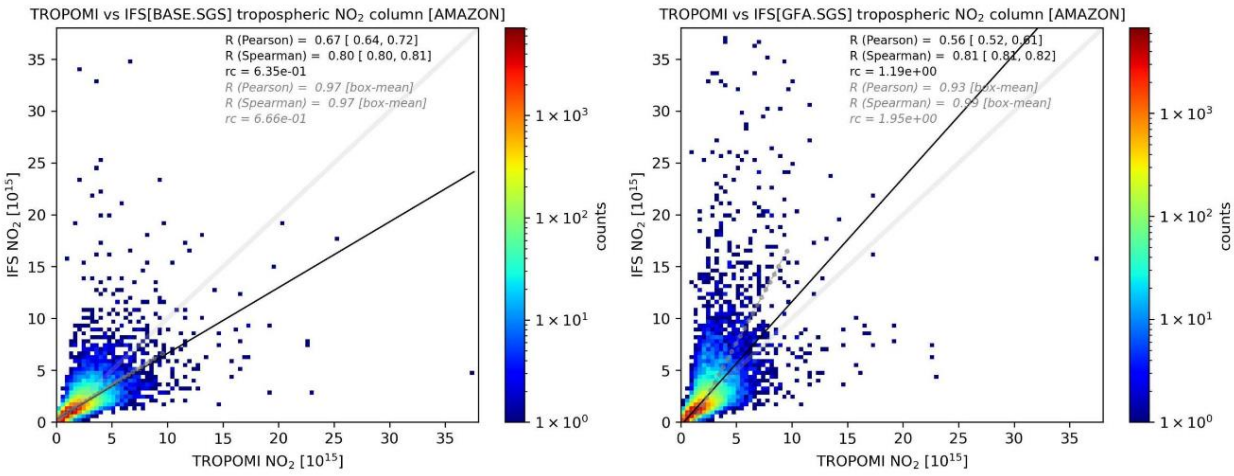

Figure 5: August-September 2020 Amazon/Cerrado probability distribution of daily TROPOMI observed (x-axis) and collocated IFS-COMPO simulated (y-axis) tropospheric NO2 columns for the simulation using GFAS emissions (BASE; left panel) and GFA-S4F emissions (rig right panel). Note the logarithmic color scaling. The solid grey line is the 1:1 line, the black line a linear regression (statistics displayed in the plot), the grey line with markers displays the regression results after first averaging data in distinct intervals (binning).

For CO there similarly is a good agreement between TROPOMI observations and IFS-COMPO model results (Figure 6). There are some indications that GFAS underestimates CO emissions, like the distribution tail of high TROPOMI CO column values not reproduced by IFS-COMPO. However, the core of the distribution shows a good agreement and is better than with the GFAS version used in the PVRv2 and in de Laat et al. (2024). Still, the GFA data shows a better agreement with IFS-COMPO and results than GFAS. Note that monthly data shows that outside of the fire season CO is biased high in IFS-COMPO (thus not fire related). The higher CO columns point at higher fire emissions in GFA-S4F, as seen in the time series of daily CO emissions (Figure 6). Indeed, this figure show that GFAS and GFA-S4F agree on the temporal changes – just like for NO_x - but that GFA-S4F emissions are in total approximately 50% higher than in GFAS.

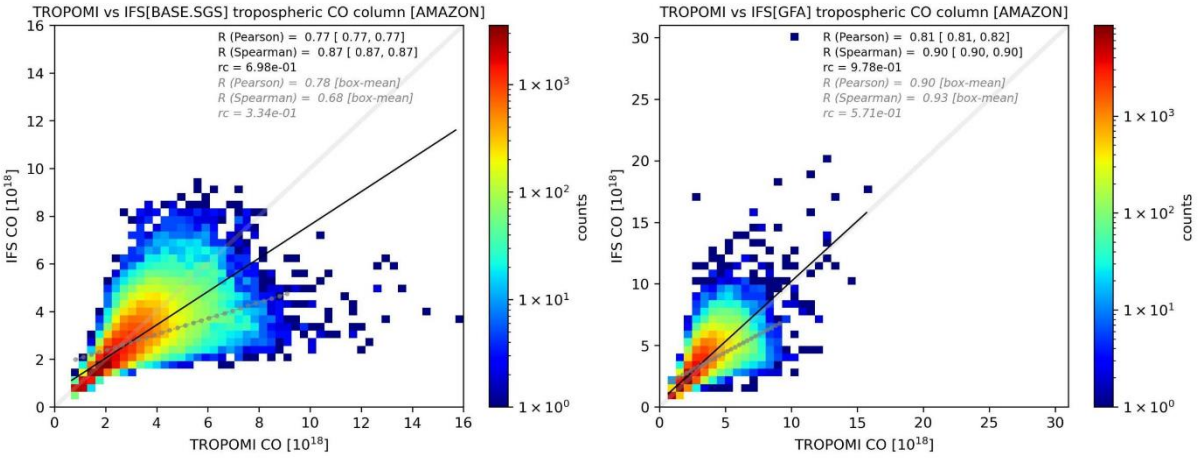

Figure 6: As Figure 2.3.2 but for CO for August-September 2020.

4 Southern Africa

4.1 Validation of GFA-S4F

For southern hemisphere Africa we compared our burned area estimates to those of GFED5 (Chen et al., 2023). The GFED5 burned area dataset is based on the MCD64A1 burned area product with addition of small fires from scaling against Landsat and Sentinel-2 data. For southern hemisphere Africa, GFA-S4F estimated 191.2 Mha burned area in 2020 and GFED5 222.0 Mha.

4.2 Validation of TUD-S4F

Estimated fuel load, fuel consumption and combustion completeness from TUD-S4F were for southern Africa compared with statistical distributions from field samples as compiled in van Wees et al. (2022) (W22) and by Holland et al. (2014) (Figure 7). Observations are not available for all fuel components and we here present results for fuel components with > 10 field observations.

TUD-S4F reproduces the distribution of herbaceous fuel loads but tends to overestimate the fuel load of litter and FWD (Figure 7). Median total fuel consumption matches the

observed median but TUD-S4F shows many fires with higher values of fuel consumption than included in the field data. The range of herbaceous fuel consumption agrees with field data but the median tends to be underestimated. However, from the field data it is not clear if herbaceous fuels contain dry or dead grass which would be included in the litter fuels in TUD-S4F. Total combustion completeness in the field data is concentrated around 90% with a few observations having lower or higher values. In TUD-S4F, combustion completeness ranges from 0 to 100%. This mismatch might be because mainly herbaceous fuels were considered in the field data while TUD-S4F includes also woody debris and live woody fuels in the calculation of combustion completeness and hence shows a larger variability. This hypothesis is supported by the comparison of the combustion completeness of herbaceous fuels, which show similar ranges in the field data in TUD-S4F.

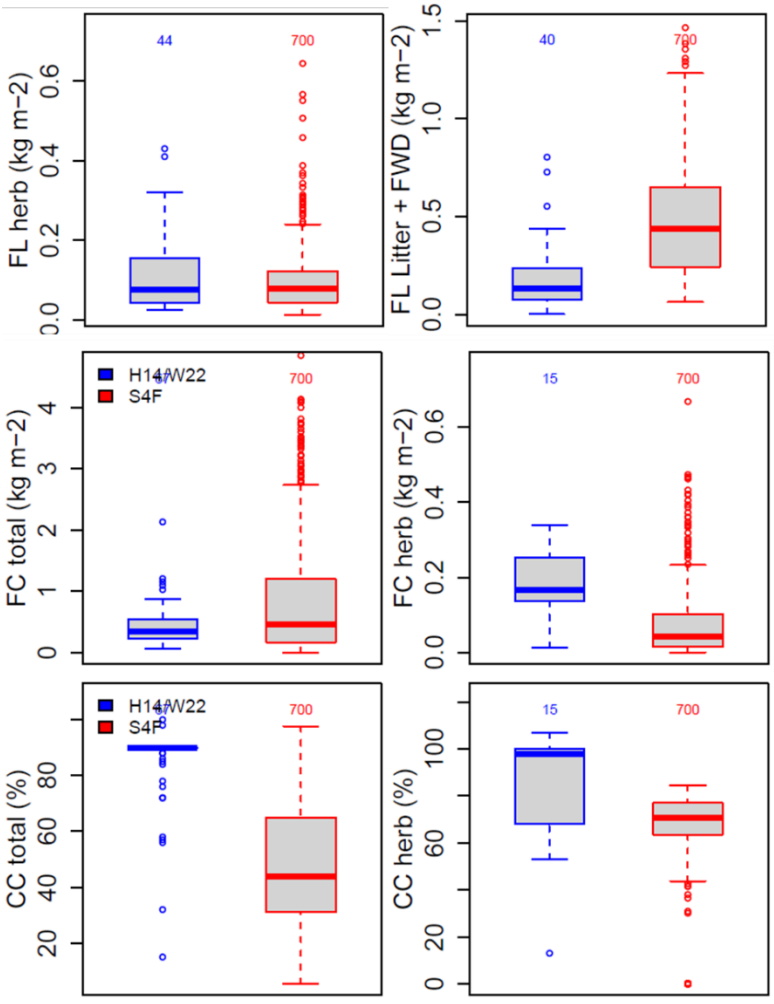

Figure 7: Comparison of distributions of fuel loads (FL), fuel consumption (FC) and combustion completeness (CC) for the Southern Africa study region from TUD-S4F with the field data included in van Wees et al. (2022) (W22, 96 sites) and Holland et al. (2014) (H14, 1 site).

Like in the Amazon/Cerrado study region, TUD-S4F also reproduces the median emission factors for CO_2, CO and the MCE as reported by Andreae (2019) in southern Africa (Figure 8). However, the results for southern Africa show a lower variability than the results for the Amazon/Cerrado. TUD-S4F seems to underestimate the emission factor for PM2.5.

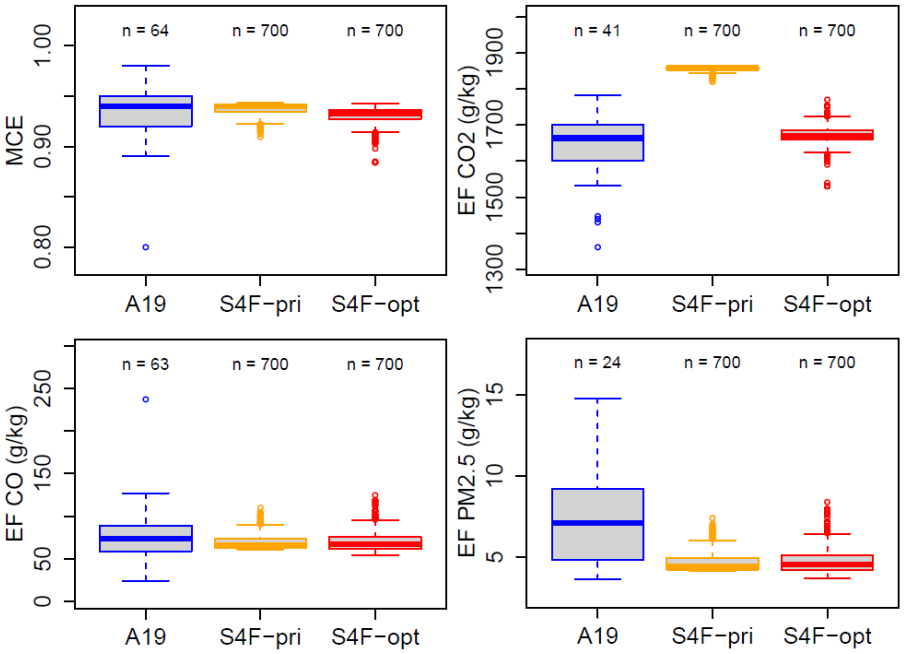

Figure 8: Comparison of modified combustion efficiency and emission factors from Andrea (2019) (for tropical forests and savannas) with results from TUD-S4F prior and after optimization for Southern Africa.

4.3 Validation against Sentinel-5p

The time series for CO and NO_x emissions for southern Africa show consistent temporal variability amongst all emission databases, but also large differences (Figure 9). Both findings are similar to what was reported for the Amazon. GFAS total CO emissions for this region for the year 2020 amount to 48 Tg, whereas GFA-S4F CO emissions are more than four times larger (213 Tg). The TUD-S4F emissions end up in the middle (102 Tg). For NO_x the 2020 total GFAS emissions amount for 1.6 Tg NO yr^{-1} whereas the equivalent GFA-S4F emissions are approximately three times larger (4.9 Tg yr^{-1}). Again, TUD-S4F ends in the middle (3.2 Tg yr^{-1}).

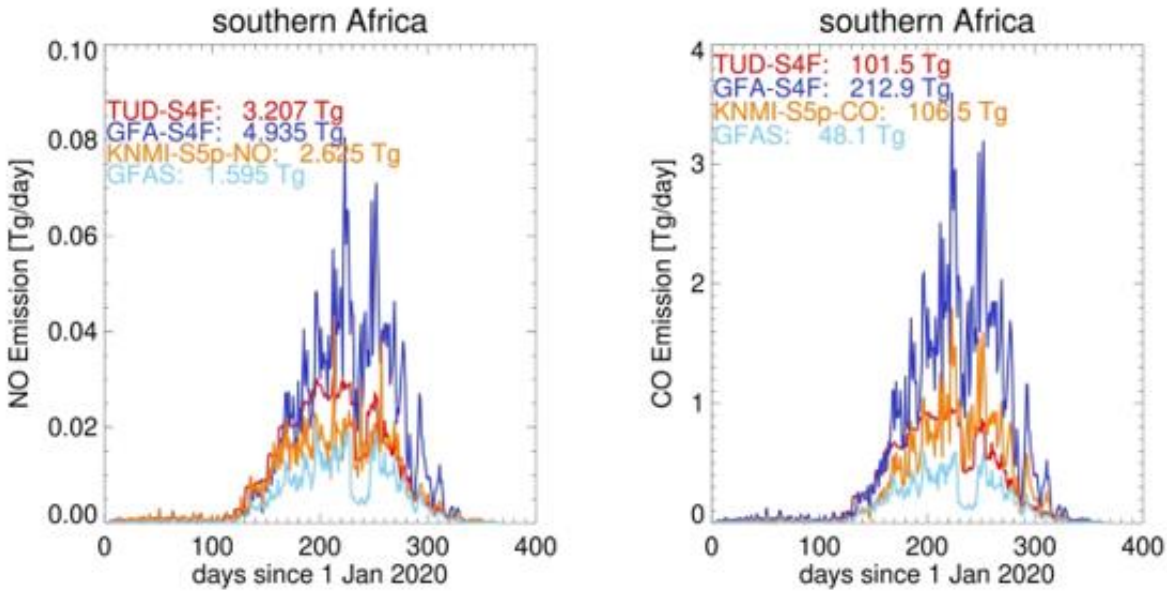

Figure 9: Daily NOx (as NO, left) and CO (right) emission estimates for sub-equatorial Africa in 2020 for the various products.

Evaluation of IFS-COMPO using the GFAS against TROPOMI NO_2 observations emissions (Figure 9, left panel) show in general a fair agreement between observed and modeled tropospheric NO_2 columns although the regression indicates an underestimation which is dominated by the distribution and dominance of smaller tropospheric NO_2 columns ($5 < 10^{15}$ molecules cm^{-2}). There is a large spread in the distribution around the 1:1 line. Overall, results are similar to the Amazon region.

For the IFS-COMPO simulations using the GFA-S4F emissions the results for sub-equatorial Africa are significantly different from those report for the Amazon. The large-fire NO_x bias is evident, even though the core of the distribution also in Africa remains close to the 1:1 line.

The KNMI-S5p optimized NO_x emissions are larger than the GFAS emissions and much smaller than the GFA-S4F emissions (Figure 9): 2.6 Tg NO yr^{-1}, when using GFA-S4F as a-priori. For reference, the KNMI-S5p optimized emissions are 2.3 Tg NO yr^{-1} with GFAS as a-priori, not shown. Like for the Amazon, the differences in the distributions are solely associated with fire emissions.

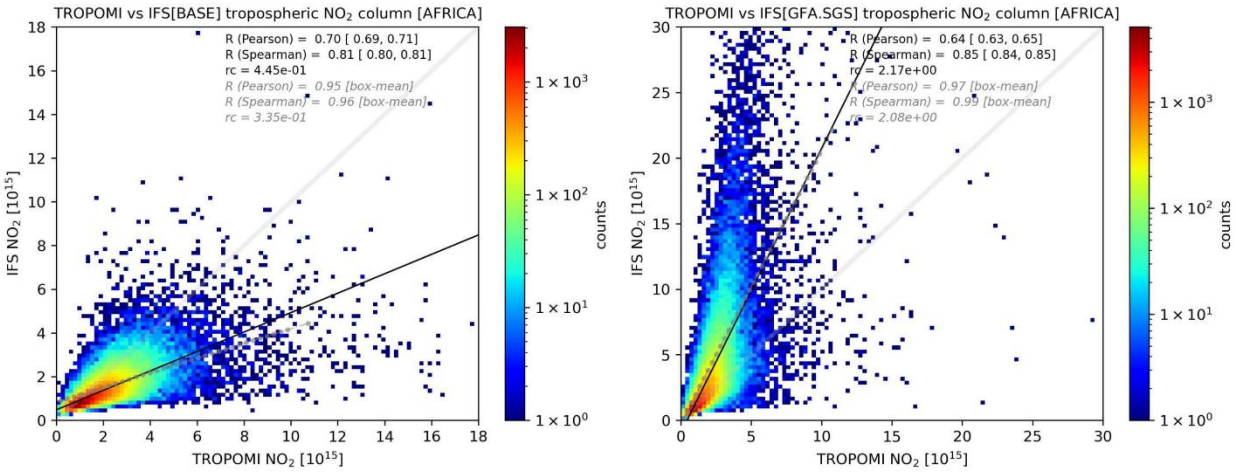

Figure 10: Pobability distribution of daily TROPOMI observed (x-axis) and collocated IFS-COMPO simulated (y-axis) tropospheric NO_2 columns for the south-equatorial African region for August-September 2020. Left: IFS-COMPO using GFAS emissions, and right using GFA-S4 emissions

For CO the there is a good correlation between observations and model results (Figure 10). However, both GFAS and GFA-S4F show clear biases with GFAS underestimating CO – as also reported for Africa in de Laat et al. (2024) and with GFA-S4F largely overestimating CO. The latter is consistent with the overestimation of NO_2 (Figure 10).

The consistent overestimation of African south-equatorial fire emissions in GFA-S4F indicate problems with the conversion of satellite information (Fire Radiative Power, Burned Area) to emission rates. This is unsurprising, as the GFA-S4F algorithm has not been tuned with known fire emission factors – especially for woodland and forests.

A test with halving GFA-S4F emissions for CO towards 107 Tg yr^{-1} (Figure 9), denoted as KNMI-S5p CO emissions, indeed results in a good match of IFS-COMPO simulations with TROPOMI CO observations, with a slope that is close to unity (Figure 12). These emission estimates were derived from the biases uncovered previously, and yields results closer to the TUD-S4F CO emissions. The TUD-S4F algorithm derive their emission factors from satellite-data-based estimates of fuel loads, fuel moisture and soil moisture and prove more realistic than the current emission factors used in GFA-S4F for sub-equatorial Africa. Note that the comparison of IFS-COMPO simulations with the original GFA-S4F CO emissions over this region suggest that the scaling factor may be slightly more than halving the CO emissions (0.40-0.45). This was not explored further, also because the halving of the emissions (0.5) was already a post-hoc test. However, it suggests that – unlike for NOx – no sophisticated approaches are needed for determining first order updates of CO emissions.

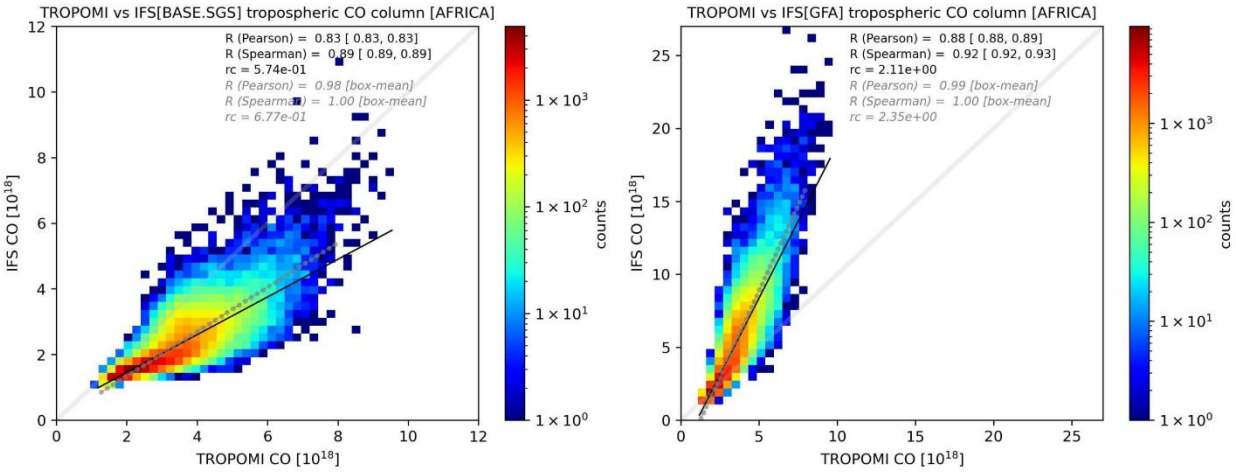

Figure 11: Probability distribution of daily TROPOMI observed (x-axis) and collocated IFS-COMPO simulated (y-axis) tropospheric CO columns for the south-equatorial African region for August-September 2020. Left: IFS-COMPO using GFAS emissions, and right using GFA-S4F emissions.

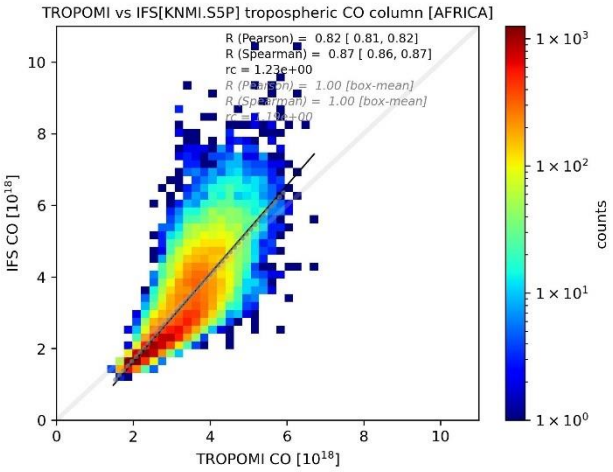

Figure 12: Probability distribution of daily TROPOMI observed (x-axis) and collocated IFS-COMPO simulated (y-axis) tropospheric CO columns for south-equatorial African region for August-September 2020 for the simulation using KNMI-S5p emissions.

5 Siberia

5.1 Validation of GFA-S4F

We have not revised our validation for the Siberia region since the PVR2.1.

5.2 Validation of TUD-S4F

Estimated fuel load, fuel consumption and combustion completeness from TUD-S4F were for Siberia compared with statistical distributions from field samples as compiled in van Wees et al. (2022) (W22). Observations are not available for all fuel components and we here present results for fuel components with > 10 field observations.

TUD-S4F tends to underestimate the fuel load of living vegetation (wood, leaves) but corresponds well to the observed distribution of woody debris and litter and fine woody

debris (Figure 13). The underestimation of living fuel loads could be due to the fact that most of the field data in W22 originates from regions the west of the Siberia test area which has generally a higher biomass than the forests within the Siberia test area. Hence a more spatially aligned comparison of fuel loads requires more field observations.

The differences in fuel loads translate into similar differences in fuel consumption. TUD-S4F tends to underestimate total fuel consumption but agrees with the fuel consumption of woody debris and litter.

Estimated combustion completeness agrees between TUD-S4F and the values compiled in W22 for most fuel components but for litter and fine woody debris. The latter is likely due to the fact that in the field data mainly high severity ground fires were sampled whereby TUD-S4F includes fire burning under several conditions.

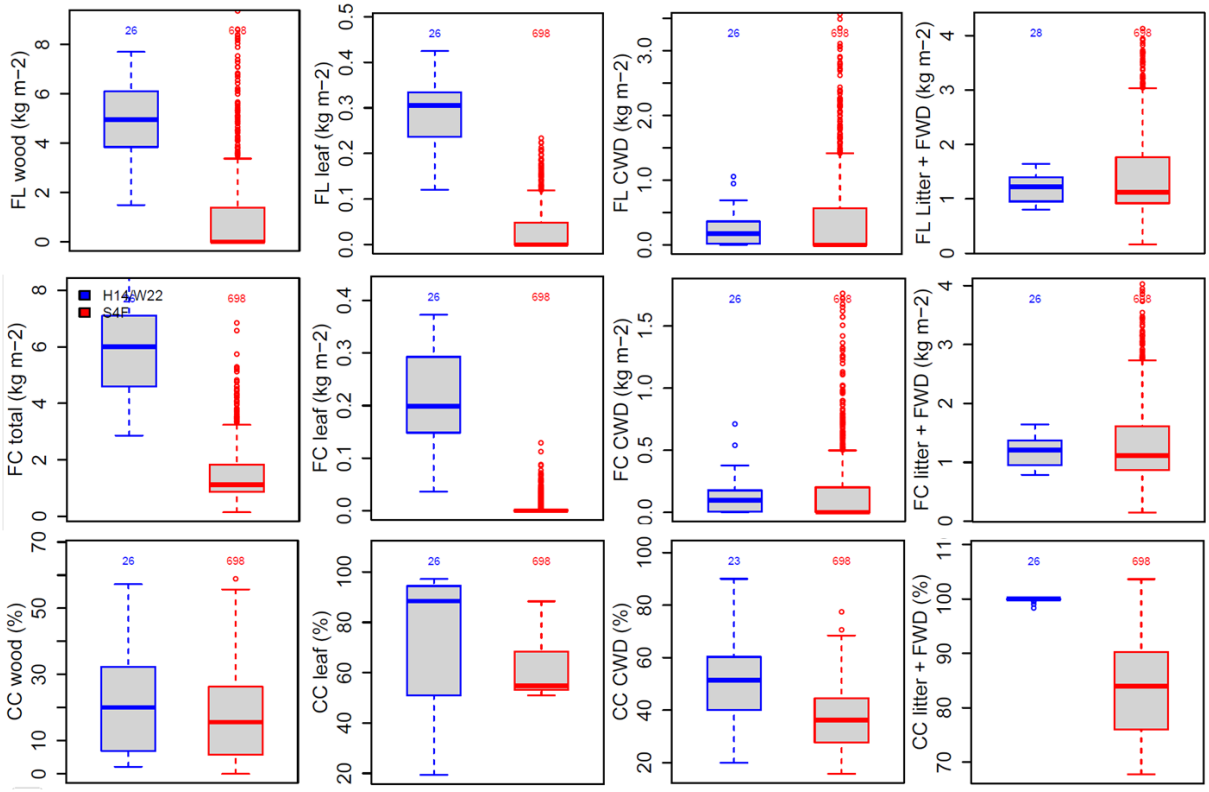

Figure 13: Comparison of distributions of fuel loads (FL), fuel consumption (FC) and combustion completeness (CC) for the Siberia test area from TUD-S4F with the field data included in van Wees et al. (2022) (W22, 26 sites) and Holland et al. (2014) (H14, 3 sites).

5.3 Validation against Sentinel-5p

The time series of emissions (Figure 14) show that fire emissions occur much more sporadic resulting in a more stochastic time series, with fires found mostly in the months July-September. The total 2020 NO_x emissions for GFAS (74 Gg) are higher than for TUD-S4F (55 Gg) and GFA-S4F (15 Gg); note that for these boreal fires the default GFAS NO_x emissions have been scaled down by a factor 0.34, because of a known outdated emission factor specifically for NO_x. The corresponding CO emissions are more similar (2.29 Tg for

GFAS, 2.17 for GFA-S4F, 2.03 for TUD-S4F), with GFA-S4F showing higher peak emission values in combination with lower values in case of smaller fires, compared to GFAS.

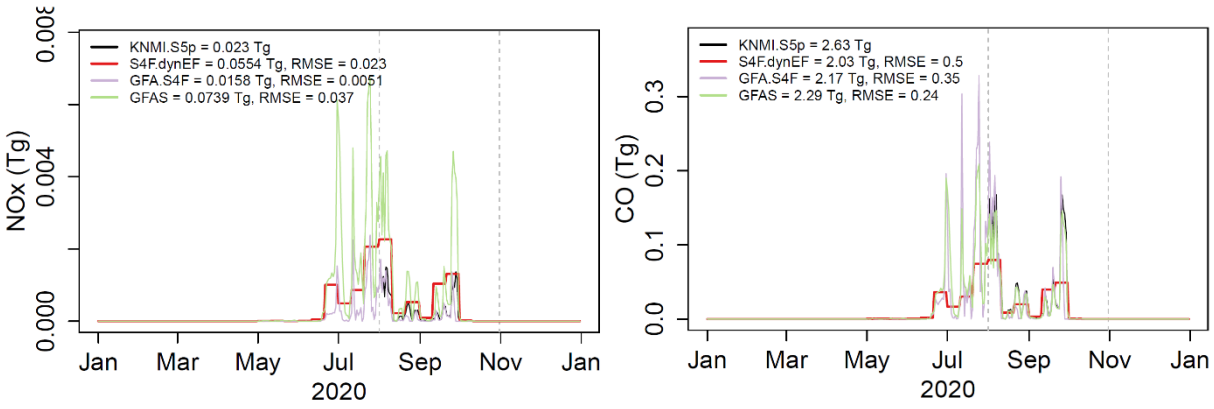

Figure 14: Daily NOx (as NO, left) and CO (right) emission estimates for the Siberia Taiga/Tundra region in 2020 for the various products.

Evaluation results of IFS-COMPO versus TROPOMI observations for the Siberia region are more difficult to interpret than those for the Amazon/Cerrado and sub-equatorial Africa regions due to many fewer fires occurring. Figure 15 nevertheless displays indications of also here a large-fire NO_x bias particularly in the GFA-S4F dataset, which is confirmed by a more detailed analysis (not shown).

The β-optimization cannot resolve this discrepancy (Figure 14), likely due to fewer fires and more cloudiness, limited the possibility for using TROPOMI measurements for the post-hoc emission adjustment.

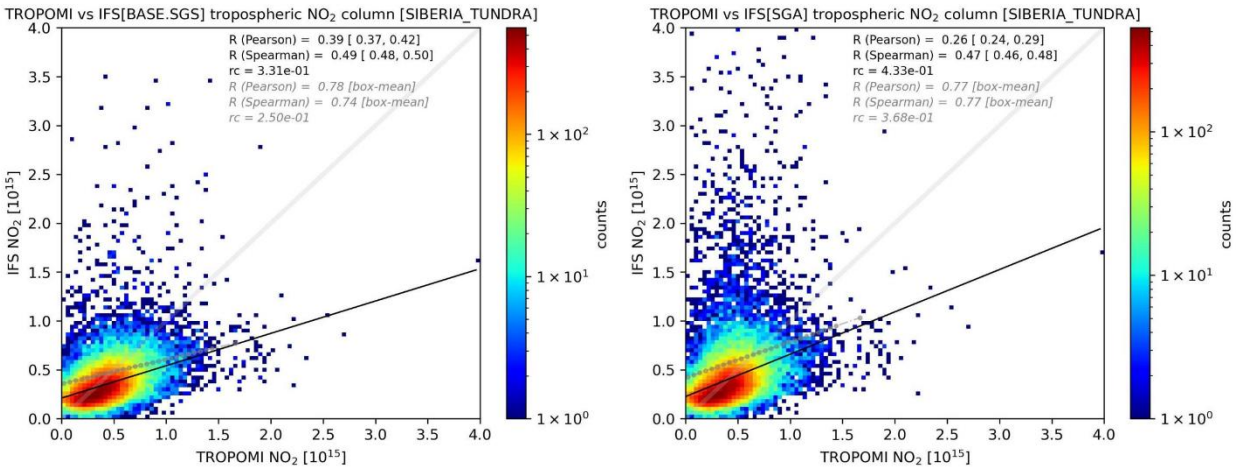

Figure 15: Probability distribution of daily TROPOMI observed (x-axis) and collocated IFS-COMPO simulated (y-axis) tropospheric NO2 columns for the Siberian Taiga/Tundra region in August-September 2020. Left: IFS-COMPO using GFAS emissions, and right using GFA-S4F emissions.

For CO, the results are similar to those of NO_x in the sense that differences in the probability distributions are marginal (Figure 16). Both GFAS and GFA-S4F appear to

underestimate fire CO emissions which is consistent with what is reported in de Laat et al. (2024), although the GFA-S4F emissions appear to capture slightly better the large fire events, indicated by a better slope in the regression line, and improved correlation.

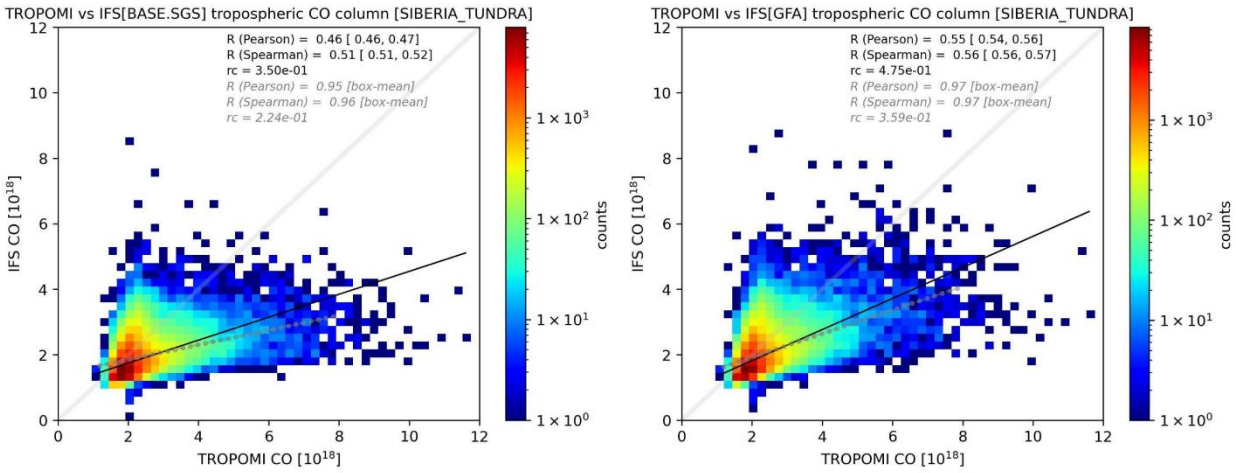

Figure 16: Probability distribution of daily TROPOMI observed (x-axis) and collocated IFS-COMPO simulated (y-axis) tropospheric CO columns for the Siberian Taiga/Tundra region in August-September 2020. Left: IFS-COMPO using GFAS emissions, and right using GFA-S4F emissions.

6 Europe

6.1 Validation of GFA-S4F

For the European study region, we compared our burned area estimates to those of GFED5 (Chen et al., 2023). The GFED5 burned area dataset is based on the MCD64A1 burned area product with addition of small fires from scaling against Landsat and Sentinel-2 data. For the European study region, GFA.S4F estimated 4.2 Mha burned area in 2020 and GFED5 3.1 Mha.

6.2 Validation of TUD-S4F

Validation of fuel load and fuel consumption from TUD-S4F over Europe is more challenging than in the other regions because the fuel consumption database by van Wees et al. (2022) contains only a few measurements. Hence for the comparison over Europe, we mainly take observation from the Database of Litter Fall Masses and Litter carbon (Holland et al., 2014). The comparison of litter and the combined litter and FWD show that TUD-S4F reproduces plausible ranges but has a tendency to overestimate litter loads over Europe (Figure 17).

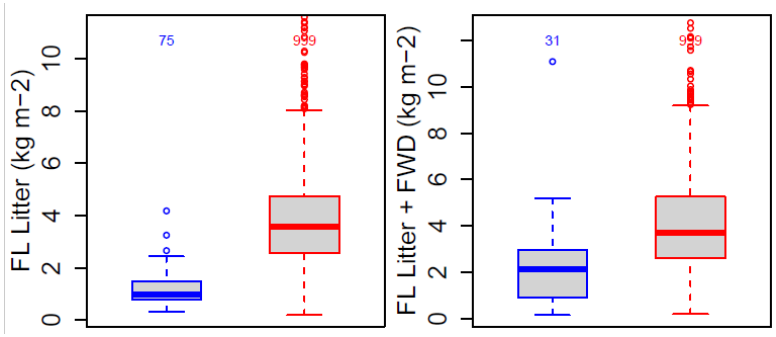

Figure 17: Comparison of litter fuels and litter and FWD from field data by Holland et al. (2012) and from TUD-SF4.

The comparison of MCE and emission factors for Europe with the values reported by Andreae (2019) for temperate forests shows that TUD-S4F reproduces median values but tends to underestimate the variability of emission factors (Figure 18).

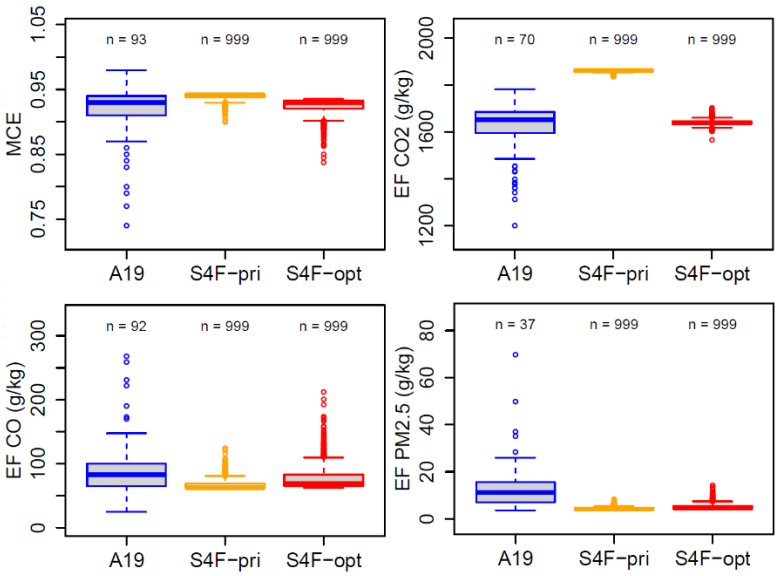

Figure 18: Comparison of modified combustion efficiency and emission factors from Andrea (2019) (for temperate forests) with results from TUD-S4F prior and after optimization for Europe..

6.3 Validation against Sentinel-5p

For the southern Europe region only the months August and September 2020 were analyzed. The emissions time series shows large differences between 2020 total GFAS NO_x emissions (33 Gg) and GFA-S4F emissions (105 Tg). Also the GFA-S4F CO emissions are much larger (4.4 Tg CO yr^{-1}) than those estimated by GFAS (1.0 Tg CO yr^{-1}).

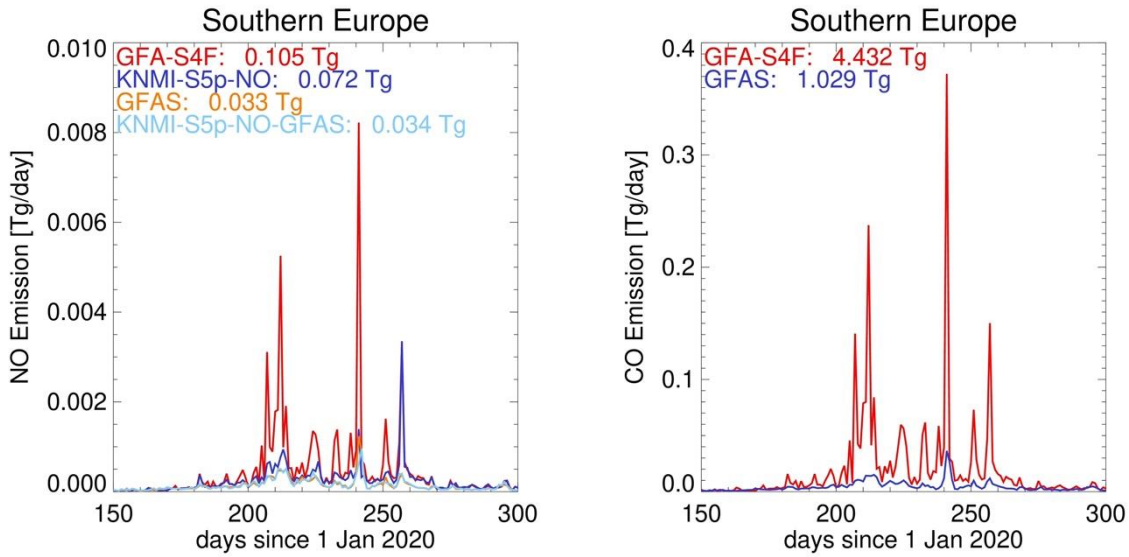

Figure 19: Daily NOx (as NO, left) and CO (right) emission estimates for Southern Europe/Mediterranean region in June-October 2020 for the various products.

Figure 20 shows the probability distributions of observed and modeled tropospheric NO_2 columns. Despite the limited number of fires there is a clear indication of also here large-fire NO_x bias in GFA-S4F, not present in GFAS. The overall NO_2 bias in both simulations is unrelated to fire emissions.

The β-optimization has limited impact on the GFAS emissions but reduces the GFA-S4F emissions, a possible indication that GFAS emissions could be closer to reality than GFA-S4F emissions. However, this is speculative as the number of fires and thus data to constrain fire emissions in this regions is limited; the optimized emissions remain rather dependent to the prior emissions.

For CO there clearly is a large positive bias in GFA-S4F fire emissions (Figure 21). This is consistent with the results for NO_x and similar to what was seen for sub-equatorial Africa.

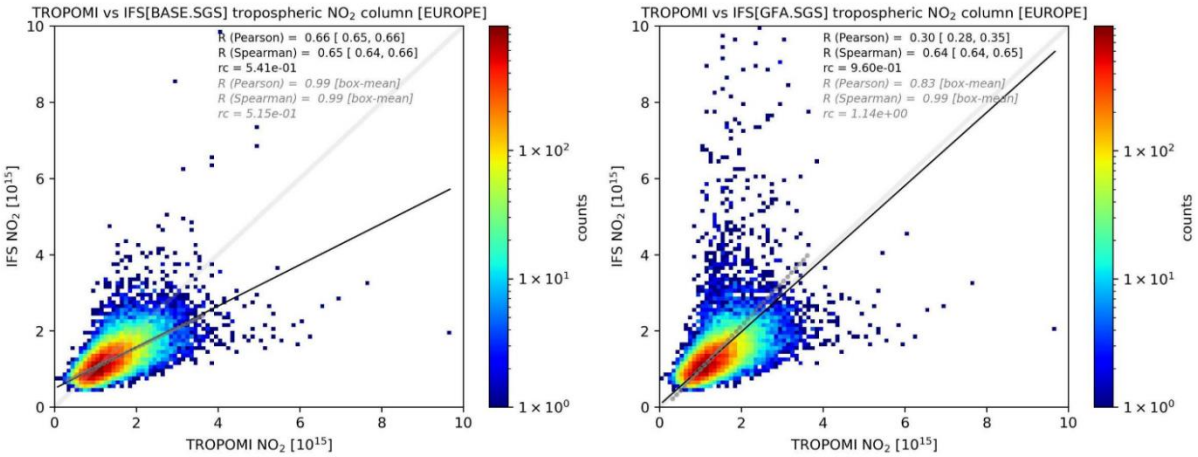

Figure 20: Probability distribution of daily TROPOMI observed (x-axis) and collocated IFS-COMPO simulated (y-axis) tropospheric NO2 columns for the Southern Europe region for August 2020. Left: IFS-COMPO using GFAS emissions, and right using GFA-S4F emissions

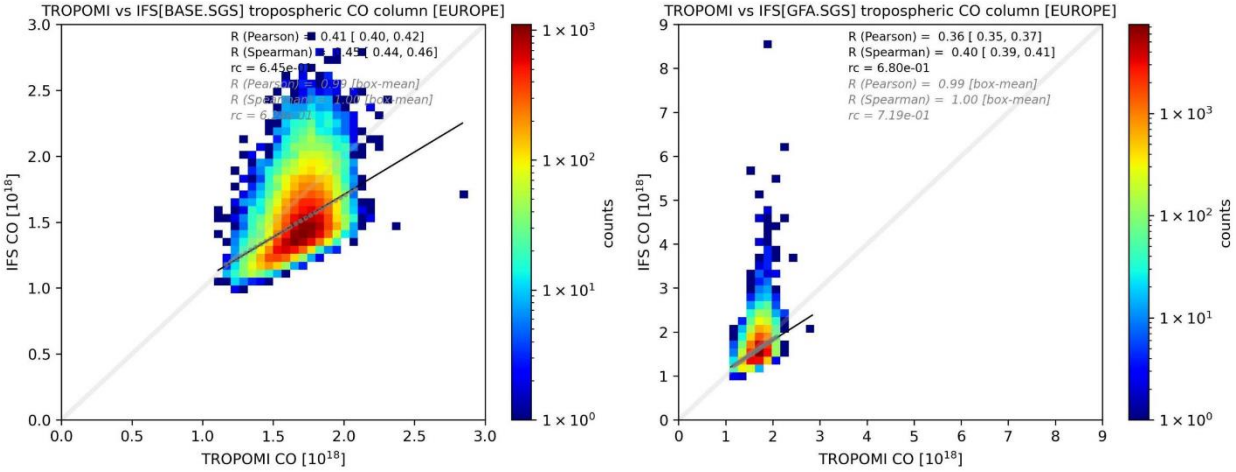

Figure 21: Probability distribution of daily TROPOMI observed (x-axis) and collocated IFS-COMPO simulated (y-axis) tropospheric CO columns for the Southern Europe region for August 2020. Left: IFS-COMPO using GFAS emissions, and right using GFA-S4F emissions. Note the different vertical axis range in both plots.

Although there were limited number of (large) fires over Europe in 2020, there is one particular appealing fire case on 29 and 30 August 2020 that illustrates the far-reaching effects fires in Europe can have – even if incorrectly represented in the IFS-COMPO model.

Figure 22 shows TROPOMI observed and IFS-COMPO simulated tropospheric NO_2 columns and total CO columns using GFA-S4F emissions. The GFA-S4F NO_2 results indicates a large fire occurring on 29 August 2020 over northern Algeria and its border with Tunesia. The TROPOMI data do show enhanced NO_2 as well but by far not as much as in the IFS-COMPO model simulation.

Comparing the tropospheric NO_2 columns and CO total columns over central Europe one day later reveals strong enhancements of both parameters over central Europe (Croatia and Hungary) at the leading edge of a frontal zone recognizable as a band without data. Those enhancements, however, are not found in the TROPOMI data. Such long-range

transport of fire emission plumes is typical for the middle and high latitudes which is much less common over equatorial regions.

In this particular case the β-optimization indeed can reduce the NO_x emissions over northern Algeria. However, would the fire have remained undetected by TROPOMI the emissions would not have been adjusted. This case thus also nicely reveals the limitations of the β-optimization. A more formal emission inversion algorithm might have been able to reduce the emissions from observations made later in time.

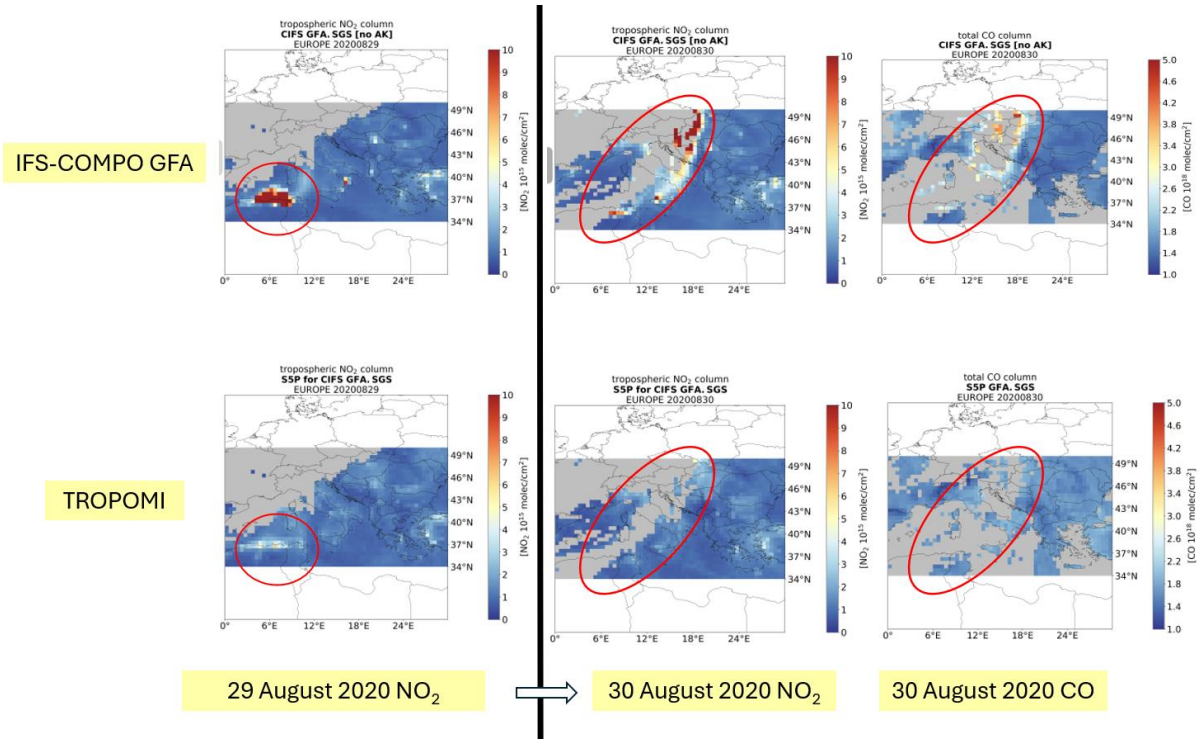

Figure 22: TROPOMI observations (lower panels) for 29 August 2020 and corresponding IFS-COMPO simulation using GFA-S4F fire emissions simulation results (upper panels) and (NO2, left panels) and 30 August 2020 (NO2, middle panels; CO, right panels). The red circles indicate the fires on 29 august 2020 and the transported emission plume on 30 august 2020 in the IFS-COMPO simulations and weaker enhancements or lack of enhancements in TROPOMI observations.

7 Summary

The top-down approaches using retrievals of atmospheric composition in combination with IFS-COMPO simulations clearly reveal the added value of using TROPOMI data and model simulations to constrain bottom-up emissions. Overall, the evaluations reveal that a good spatio-temporal agreement can be found for both GFA-S4F and TUD-S4F but also that for certain regions large biases exist (e.g. overestimation of emission by GFA-S4F in southern Africa). For GFA-S4F these are likely related to missing region-specific (and thus biome specific) information on vegetation characteristics, including local emission factors.

Likewise, results show that TROPOMI observations can also be used to estimate fire emissions, provided there are sufficient observations to constrain them. Here this is done by applying the so-called β-optimization, which works as post-hoc consistency check for NO_x emissions. For CO emissions it appears sufficient to apply emission changes based on budget considerations (differences in CO total columns).

Compared to these TROPOMI-based optimized emissions, the TUD-S4F emissions appear well in line, giving at least confidence in their annual totals and seasonal cycle. This suggest the benefit of including the dynamically calculated emissions factors along with vegetation information like fuel load, fuel moisture and soil moisture.

The use of TROPOMI observations can in future be expanded for determining specific individual fire emission factors.

References

Andela, N., Morton, D. C., Giglio, L., Paugam, R., Chen, Y., Hantson, S., Van Der Werf, G. R., and Randerson, J. T.: The Global Fire Atlas of individual fire size, duration, speed and direction, Earth Syst. Sci. Data, 11, 529–552, 2019.

Andela, N., Morton, D. C., Schroeder, W., Chen, Y., Brando, P. M., and Randerson, J. T.: Tracking and classifying Amazon fire events in near real time, Sci. Adv., 8, eabd2713, https://doi.org/10.1126/sciadv.abd2713, 2022.

Andreae, M. O.: Emission of trace gases and aerosols from biomass burning–an updated assessment, Atmospheric Chem. Phys., 19, 8523–8546, 2019.

Chen, Y., Hall, J., van Wees, D., Andela, N., Hantson, S., Giglio, L., van der Werf, G. R., Morton, D. C., and Randerson, J. T.: Multi-decadal trends and variability in burned area from the fifth version of the Global Fire Emissions Database (GFED5), Earth Syst. Sci. Data, 15, 5227–5259, https://doi.org/10.5194/essd-15-5227-2023, 2023.

Forkel, M., Andela, N., de Laat, J., Huijnen, V., Awotwi, A., Kinalczyk, D., Marrs, C., and Wessollek, C.: Sense4Fire ATBDv2.1. Sentinel-based fuel, fire and emissions products to constrain the changing role of vegetation fires in the global carbon cycle. Algorithm Theoretical Baseline Document Version 2.1, 2023.

Forkel, M., Andela, N., de Laat, J., Huijnen, V., van Wees, D., Kinalczyk, D., Marrs, C., and Wessollek, C.: Sense4Fire ATBDv3. Sentinel-based fuel, fire and emissions products to

constrain the changing role of vegetation fires in the global carbon cycle. Algorithm Theoretical Baseline Document Version 3, 2024.

Holland, E. A., Post, W. M., Matthews, E. G., Sulzman, J. M., Staufer, R., and Krankina, O. N.: A Global Database of Litterfall Mass and Litter Pool Carbon and Nutrients, , https://doi.org/10.3334/ORNLDAAC/1244, 2014.

Kaiser, J. W., Heil, A., Andreae, M. O., Benedetti, A., Chubarova, N., Jones, L., Morcrette, J.-J., Razinger, M., Schultz, M. G., Suttie, M., and van der Werf, G. R.: Biomass burning emissions estimated with a global fire assimilation system based on observed fire radiative power, Biogeosciences, 9, 527–554, https://doi.org/10.5194/bg-9-527-2012, 2012.

de Laat, A., Huijnen, V., Andela, N., and Forkel, M.: Assessment of satellite observation-based wildfire emissions inventories using TROPOMI data and IFS-COMPO model simulations, EGUsphere, 1–81, https://doi.org/10.5194/egusphere-2024-732, 2024.

Leite, R. V., Silva, C. A., Broadbent, E. N., Amaral, C. H. do, Liesenberg, V., Almeida, D. R. A. de, Mohan, M., Godinho, S., Cardil, A., Hamamura, C., Faria, B. L. de, Brancalion, P. H. S., Hirsch, A., Marcatti, G. E., Dalla Corte, A. P., Zambrano, A. M. A., Costa, M. B. T. da, Matricardi, E. A. T., Silva, A. L. da, Goya, L. R. R. Y., Valbuena, R., Mendonça, B. A. F. de, Silva Junior, C. H. L., Aragão, L. E. O. C., García, M., Liang, J., Merrick, T., Hudak, A. T., Xiao, J., Hancock, S., Duncason, L., Ferreira, M. P., Valle, D., Saatchi, S., and Klauberg, C.: Large scale multi-layer fuel load characterization in tropical savanna using GEDI spaceborne lidar data, Remote Sens. Environ., 268, 112764, https://doi.org/10.1016/j.rse.2021.112764, 2022.

Scaranello, M. A. S., Keller, M., Longo, M., dos-Santos, M. N., Leitold, V., Morton, D. C., Pinagé, E. R., and Espírito-Santo, F. D. B.: Estimation of coarse dead wood stocks in intact and degraded forests in the Brazilian Amazon using airborne lidar, Biogeosciences, 16, 3457–3474, https://doi.org/10.5194/bg-16-3457-2019, 2019.

van Wees, D., van der Werf, G. R., Randerson, J. T., Rogers, B. M., Chen, Y., Veraverbeke, S., Giglio, L., and Morton, D. C.: Global biomass burning fuel consumption and emissions at 500 m spatial resolution based on the Global Fire Emissions Database (GFED), Geosci. Model Dev., 15, 8411–8437, https://doi.org/10.5194/gmd-15-8411-2022, 2022.